

Mantle Exhumation in an Early Paleozoic Passive Margin, Northern Cordillera, Yukon

D. Canil,¹ S. T. Johnston, K. Evers, J. G. Shellnutt, and R. A. Creaser²

*School of Earth and Ocean Sciences, University of Victoria, P.O. Box 3055, 3800 Finnerty Road, Victoria, British Columbia V8W 3P6, Canada
(e-mail: dcanil@uvic.ca)*

ABSTRACT

Orogenic peridotite occurs as a megaboudin structurally juxtaposed with smaller boudined masses of corona troctolite, skarn, and garnet amphibolite in metasedimentary rocks of the Yukon-Tanana Terrane, Yukon. The peridotite shows well-developed plagioclase coronae on spinel and records cooling from $\sim 1000^\circ$ to 600°C and decompression across the spinel-plagioclase peridotite facies boundary at ~ 0.7 GPa. The troctolite boudins record cooling to 850°C through the same facies reaction at ~ 0.8 GPa. In an aureole surrounding the peridotite body, the mainly quartzofeldspathic country rock contains leucosome with garnet, orthopyroxene, and sillimanite formed from breakdown of biotite, which records temperatures of $\sim 900^\circ\text{C}$ at pressures of at least 0.7 GPa. Exhumation of the peridotite body from the mantle during rifting of continental lithosphere at least 25 km thick subjected continental margin metasediments to conditions above the fluid-absent metapelite solidus. The contrasting strength of upper mantle and crustal lithologies during extension may explain the structural juxtaposition and boudinage of upper mantle peridotite and troctolite on various scales. The Os isotopic compositions of the peridotite body show that it represents either relatively young mantle lithosphere with an age only slightly older than the Devonian metasedimentary rocks in which it is hosted or mantle that is metasomatized in the same events related to rifting. The rocks in the study area bear striking similarities to those in and surrounding the Zabargad (Red Sea) and Ronda (Spain) peridotite massifs and are interpreted to have formed in an Early Paleozoic preoceanic rift. Other enigmatic mantle tectonite occurrences in continental margin metasediments in Yukon and Alaska may have a similar origin.

Introduction

Passive margins mark the site where continents have rifted, giving rise to new ocean basins (Whitmarsh and Sawyer 1996). Geological and geophysical observations from both active and ancient rifted margins (Wernicke 1985; Whitmarsh and Sawyer 1996) can be evaluated using both theoretical (Latin and White 1990) and laboratory analog models (Brun and Beslier 1996). The transition from rifted continental margin to ocean basin is nonetheless still incompletely understood. Questions remain regarding the mechanism for exhumation of deep-seated rocks on rifted margins and the presence or absence of magmatism and crustal underplating. These questions bear on the thermal and

mechanical conditions within both the crust and mantle during plate separation.

The Yukon-Tanana Terrane in the northern Cordillera contains dominantly quartzofeldspathic metasedimentary rocks with a rifted margin affinity. This largely Paleozoic terrane is interpreted as part of a pericratonic margin (Mortensen 1992) or a ribbon continent (Johnston 2001) outboard of western North America. The original rift configurations and relationships have been obscured by subsequent deformation and amphibolite-grade metamorphism during construction of a continental arc (Mortensen 1992).

In this article, a unique exposure of orogenic mantle peridotite and its associated granulite facies aureole within the Yukon-Tanana Terrane in central west Yukon is described. The tectonic juxtaposition of crustal and mantle rocks and their pressure-temperature trajectory in a rifted margin metasedimentary sequence are hitherto unrecog-

Manuscript received February 12, 2002; accepted October 6, 2002.

¹ Corresponding author.

² Department of Earth and Atmospheric Sciences, University of Alberta, Edmonton, Alberta T6G 2E3, Canada.

nized elsewhere in this terrane. The field setting, petrographic aspects, and geochemical aspects of the field area are similar to those of the continent-ocean transition in the Red Sea (Bonatti and Seyler 1987) and are expected from analogue experiments of passive margin rifting (Brun and Beslier 1996). These data provide the first clear evidence for thinning of continental lithosphere along Early Paleozoic continental margin in the northern Cordillera and elucidate the history of this orogen and the processes occurring during rifting of the continental lithosphere.

Field Area

The field area ($62^{\circ}43'N$, $137^{\circ}55'E$) is 300 km northwest of Whitehorse within unglaciated terrain of the Wolverine Creek region south of the Yukon River in the Dawson Range, west-central Yukon (fig. 1). The rocks studied are part of a package of predominantly graphitic quartzite and quartz-biotite-muscovite schist, with subordinate amphi-

bolite, calc-silicate, and meta-igneous lithologies dipping regionally to the north (Johnston and Hachey 1993) and referred to regionally as the Nasina Series (Tempelman-Kluit 1973). A minimum age for this sequence is provided by a U-Pb zircon age of 358 ± 4 Ma (Mortensen 1992; Johnston and Hachey 1993) for the Selwyn Gneiss, an east-trending 100-km-long sill-like body of granodiorite orthogneiss with K-feldspar megacrysts that intrudes the Nasina series rocks along the north margin of the study area (fig. 2; Johnston and Hachey 1993). South of the study area, orthogneiss interpreted as a sheared plutonic body that intruded the Nasina series rocks has a U-Pb zircon age of 358 ± 3.5 Ma (Johnston and Hachey 1993). Regionally, Nasina series rocks are interleaved with mafic to felsic volcanic rocks that have U-Pb zircon ages of between 365 and 347 Ma (Mortensen 1992). These constraints are consistent with the Nasina series metasediments being Late Devonian or older. All rocks in the field area have been affected by at least two periods of deformation, with original

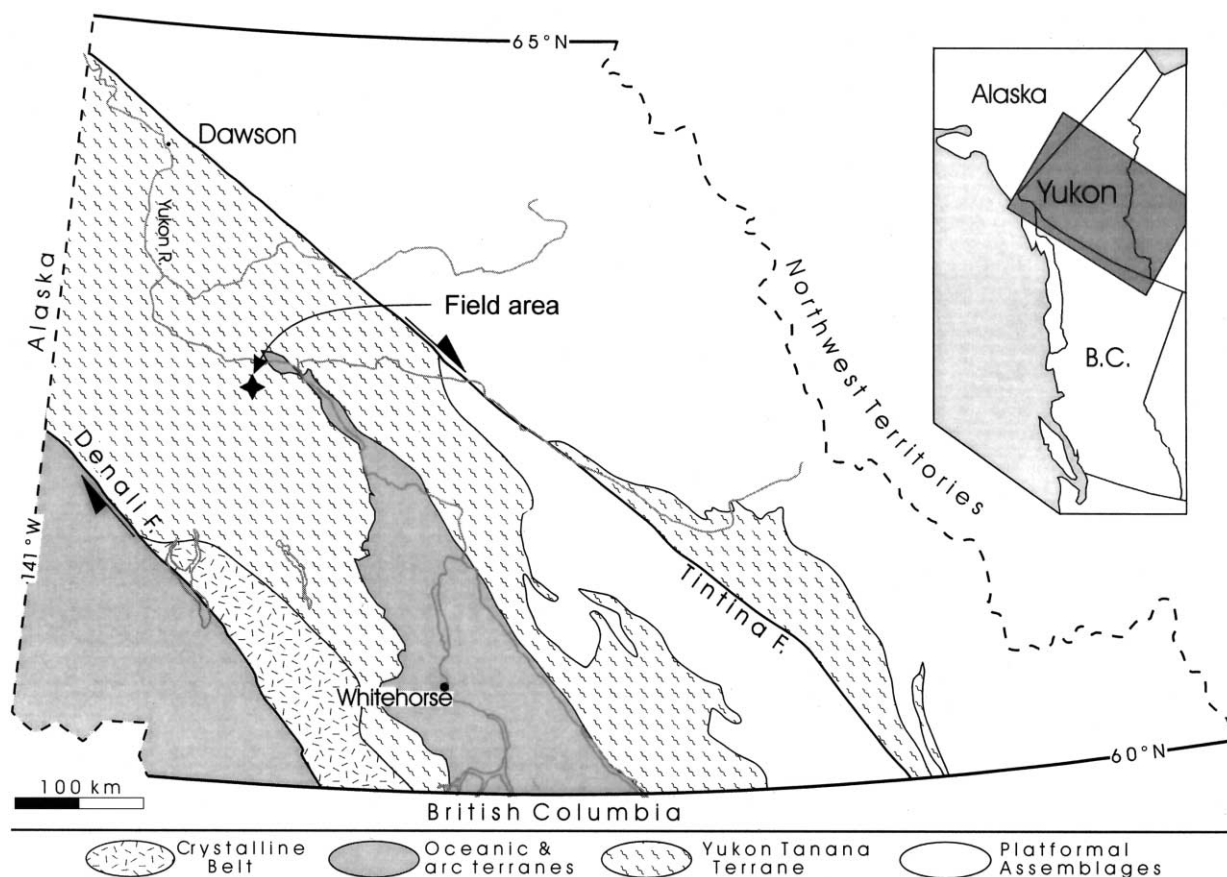


Figure 1. Regional geological map showing terranes in Yukon (Wheeler and McFeeley 1991) and location of study area north of Buffalo Pitts Mountain.

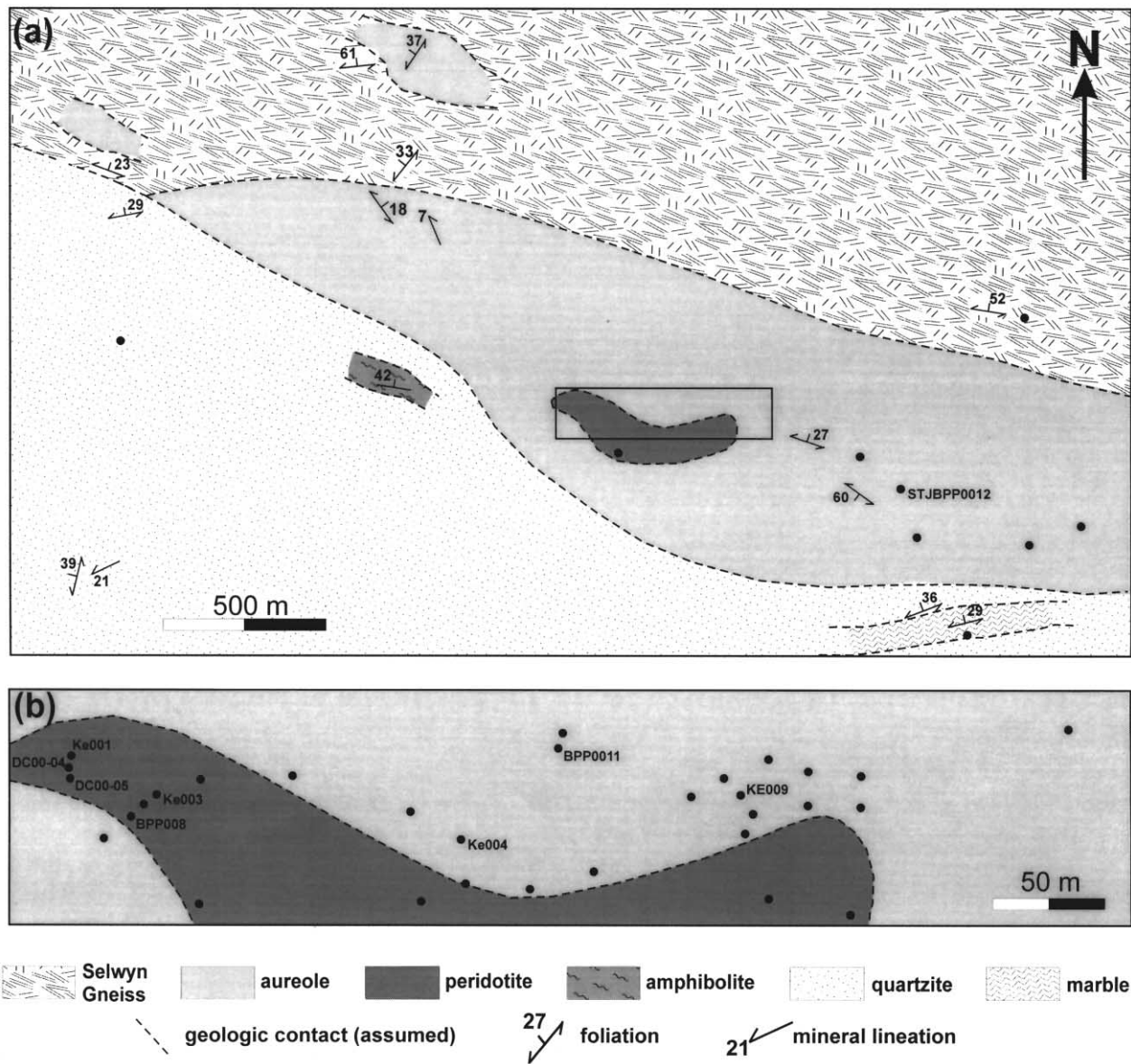


Figure 2. Geology of the field area (a) and detail of the peridotite body (b) showing sample locations (filled circles). Sample locations with analytical data discussed in this article are labeled.

stratigraphic relationships obscured by severe transposition (Johnston and Hachey 1993). Post-Mississippian brittle faulting has offset some units by tens of kilometers (Johnston 1999).

Johnston and Hachey (1993), mapping at 1 : 50,000 scale, identified an outcrop of ultramafic rock 20 km north of Buffalo Pitts Mountain (fig. 2). The ultramafic body and its wall rocks were mapped and sampled in this study at a scale of 1 : 5000. Orogenic peridotite, as defined by Den Tex (1969), is exposed as an east-trending ovoid mass 500 m long that is structurally mixed with masses

of troctolite, skarn, calc-silicate, and amphibolite in the graphitic quartzite and quartz-mica schist.

Orogenic Peridotite

The peridotite weathers dun brown and shows centimeter-scale layering defined by varying modal abundance of pyroxene and olivine similar to that described by Dick and Sinton (1979) and common to many exhumed mantle tectonites. The layering is conformable to regional foliations in the graphitic quartzite and quartz-mica schist. Millime-

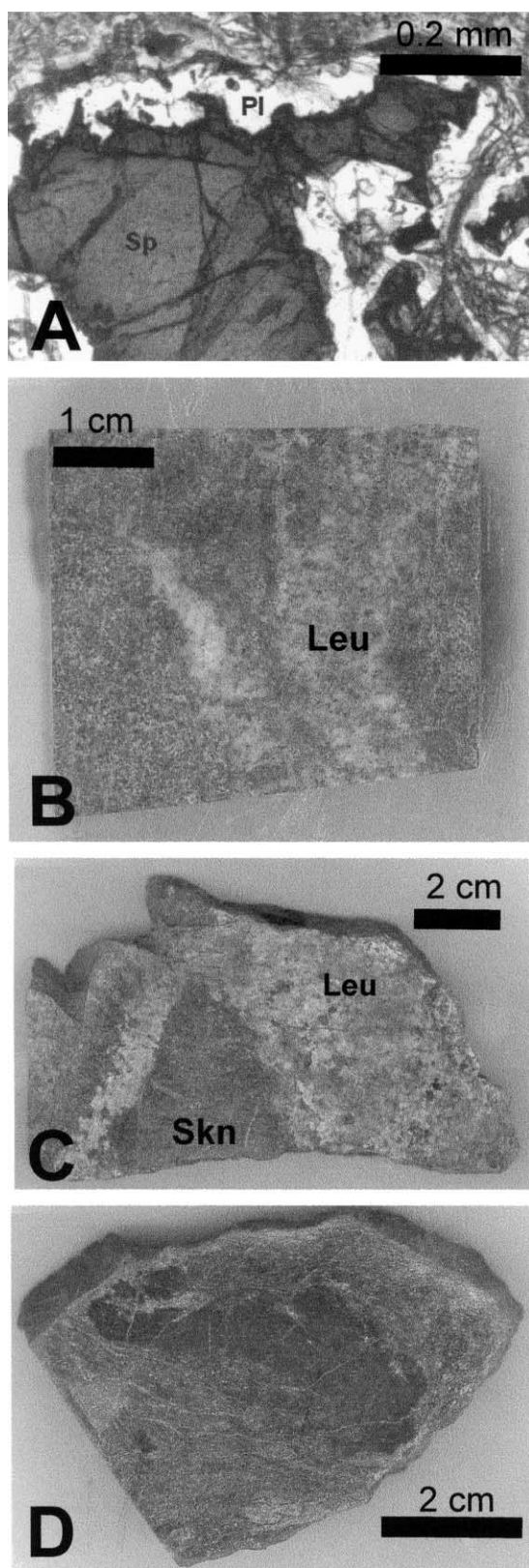


Figure 3. Scale bars shown in each panel. *A*, Photomicrograph in plane polarized light of plagioclase corona

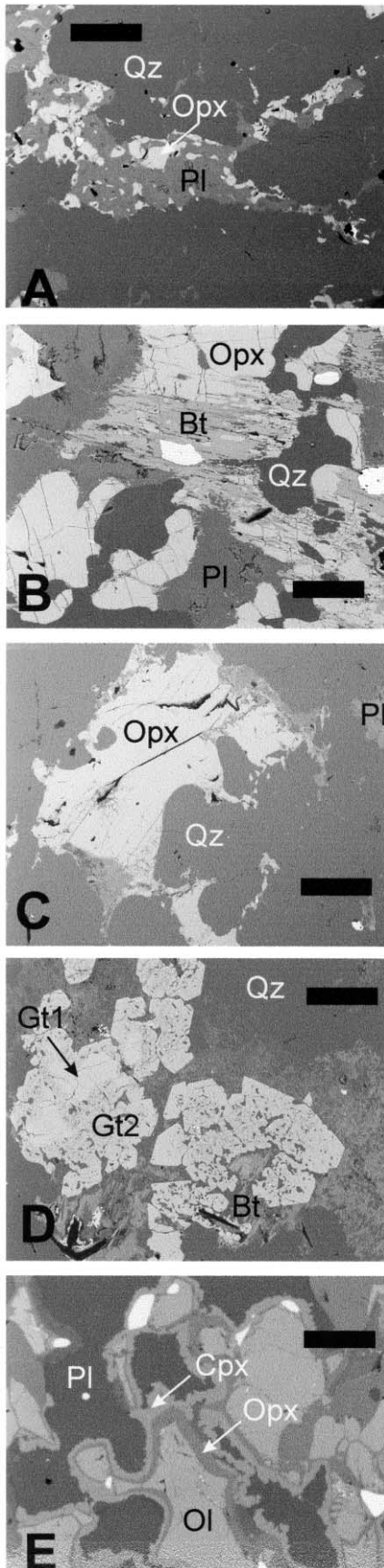
ter- to centimeter-scale veinlets of serpentine and magnetite locally crosscut the mineralogical layering and give the rock a bluish white weathered surface. Texturally, the rock is coarse lherzolite; coarse olivine is variably serpentinized (0%–70%), but coarse orthopyroxene (1–4 mm) and small grains of clinopyroxene (<1 mm) are almost always fresh and contain cores with very thin (<2 μm) exsolution lamellae. Red brown spinel is surrounded by coronae of plagioclase that weathers to a conspicuous creamy white (3A). Plagioclase (An_{77}) only occurs in these coronae and never as an interstitial phase. Phlogopite grains in textural equilibrium with other minerals are found in one sample (KE003).

In the peridotite body, olivine (Fo_{90}) is homogeneous in composition whereas orthopyroxene and clinopyroxene contain cores that are richer by a factor of 2 in CaO and Al_2O_3 than grain rims (table 1, available from *The Journal of Geology's* Data Depository upon request). The exsolution lamellae in both pyroxenes were too small to analyze by EMP. Spinel is homogeneous within individual grains but shows an increase in Mg number [$\text{Mg}/(\text{Mg} + \text{Fe})$] from 0.55 to 0.85 and a decrease in Cr number [$\text{Cr}/(\text{Cr} + \text{Al})$] from 0.48 to 0.13 with increasing grain size (0.1–1.2 mm). Phlogopite has a Mg number expected in equilibrium with the other silicate phases.

Crustal Rocks

The orogenic peridotite is intercalated at the map scale with quartzite and quartz-biotite-muscovite schist and with laterally discontinuous units of amphibolite and calc-silicate that parallel the regional foliation (fig. 2A). Within a ~400-m aureole surrounding the contact of the peridotite body, the quartzite and quartz-biotite-muscovite schist adopt a distinct blue color due to abundant accessory apatite (up to 5%). In this aureole, conspicuous centimeter-scale layers and segregations of leucosome (3B) give the country rock a heterogeneous and poorly defined gneissosity. In places, the leu-

(*Pl*) surrounding spinel (*Sp*) in peridotite body (sample KE003). *B*, Polished rock slab showing patches and veins of leucosome (*Leu*) in metapelite country rocks (KE004) of the aureole surrounding the peridotite body. *C*, Polished rock slab showing invasion and embayment of sub-angular blocks of skarn (*Skn*) by leucosome (*Leu*). *D*, Ptygmatically folded troctolite boudin in a polished slab of quartz-mica schist.



cosome intrudes or engulfs centimeter- to meter-sized subangular blocks of skarn (3C) or mafic boudins. The leucosome has granoblastic orthopyroxene (0.5–1.5 mm) and plagioclase (An₅₅) occurring in distinct pockets that appear to have wetted the surrounding quartz grains (4A, 4C). Orthopyroxene in these pockets replaces biotite (4B) and is heterogeneous in Al₂O₃ (table 1). In other places, the leucosome contains euhedral garnets (<0.1 mm) having inclusion-free, Ca-poor cores overgrown by Ca-rich rims that contain very small (<5 μm) inclusions of quartz, sillimanite, and, more rarely, orthopyroxene, all replacing biotite (4D). The appearance and proportions of sillimanite, garnet, and orthopyroxene and the composition of orthopyroxene and of plagioclase vary on the scale of a thin section in the leucosome. Sillimanite occurs elsewhere in quartzite of the aureole as subhedral, stubby prisms dispersed along cleavage planes in association with garnet and, more rarely, skeletal blue corundum.

Troctolite occurs as centimeter- to meter-scale boudins within the aureole (3D). This rock contains fine-grained (<1 mm) olivine (Fo_{45–55}) and plagioclase (An_{65–85}; table 1) overgrown by coronae of aluminous orthopyroxene and clinopyroxene, respectively, with accessory ilmenite and biotite (4E). The pyroxene coronae are fibrous at grain boundaries with olivine and plagioclase but coarsen outward to grain sizes of up to 100 μm.

Calc-silicate units occur in the aureole as blocks of skarn containing garnet-zoisite-quartz or, further afield from the peridotite body, as granoblastic

Figure 4. Backscattered electron images of rocks in the aureole surrounding the peridotite body. A, Patches of granoblastic orthopyroxene (Opx) and plagioclase (Pl) in distinct pockets between quartz grains (Qz) in leucosome from sample KE004. Scale bar is 300 μm. B, Closer view of A showing orthopyroxene (Opx), plagioclase (Pl), and quartz (Qz) overgrown on biotite (Bt) with inclusion of ilmenite (bright grain). Scale bar is 90 μm. C, Granoblastic orthopyroxene (Opx) and plagioclase (Pl) which appear to “wet” quartz grains (Qz) in sample BPP011B. Scale bar is 100 μm. D, Patches of biotite (Bt) replaced by garnet in sample BPP011B. An initial generation of garnet cores (Gt1) is overgrown by garnet rims (Gt2) containing numerous small inclusions of quartz, sillimanite, and orthopyroxene. Scale bar is 100 μm. E, Orthopyroxene (Opx) and clinopyroxene (Cpx) coronae on very fine grained olivine (Ol) and plagioclase (Pl), respectively, in a troctolite boudin (sample STJBPP12). Accessory ilmenite (bright white grains) also shown. Scale bar is 100 μm.

Table 2. Thermobarometry of Peridotites and Granulites

	T_{BKN}	T_{Tay2Px}	T_{Wells}	$T_{\text{Ca-opx}}$	$T_{\text{Al-opx}}$	$T_{\text{Ol-Sp}}$	T_{TWQ}	$P_{\text{TWQ}}^{\text{a}}$
Sample peridotites:								
KE003 rims	920	1130	940	930	900	900–650 ^b		.70
KE003 cores	920	1140	940	970	1010			
DC005 rims				960	970			
DC005 cores				1020	1020			
BPP009 rims				970	950	570		
BPP009 cores				980	990	600		
BPP008 rims				950	970			
BPP008 cores				1100	1040			
Crustal rocks:								
Boudins:								
STJBPP12	840	940					800 ^c	.80
KE009	860	950					800 ^c	.80
Crustal rocks:								
Leucosome:								
BPP011B cores							920 ^d	.85
BPP011B rims							900 ^d	.75

Note. All cation exchange thermobarometer calculations for core and rims of minerals performed at an assumed pressure of 0.8 GPa. Temperatures (T) in °C, pressures (P) in GPa. Types of thermometers used are two-pyroxene, T_{BKN} (Brey and Köhler 1990); T_{Tay2Px} (Taylor 1998); T_{Wells} (Wells 1977); Ca solubility in orthopyroxene, $T_{\text{Ca-opx}}$ (Brey and Köhler 1990); Al solubility in orthopyroxene, $T_{\text{Al-opx}}$ (Witt-Eickchen and Seck 1991); olivine-spinel Fe-Mg exchange, $T_{\text{Ol-Sp}}$ (Ballhaus et al. 1991). The temperatures (T_{TWQ}) and pressures (P_{TWQ}) from TWQ multiequilibrium calculations (Berman, 1991) represent the T and P of intersecting reactions calculated for each sample (see fig. 5).

^a From reaction (1) in text.

^b Range due to correlation with grain size of spinel.

^c From Fe-Mg exchange between two pyroxenes.

^d From Fe-Mg exchange between orthopyroxene and garnet.

calcite-quartz-tremolite-phlogopite gneiss. Discontinuous amphibolite units, also possible boudins, contain abundant large 1- to 5-mm garnets, with amphibole, epidote, and plagioclase.

The aureole of crustal rocks surrounding the peridotite body is cut by dikes of biotite granodiorite and granite with K-feldspar megacrysts. These granitoids commonly have a streaky appearance, imparted by sheared and flattened quartz-rich lenses, and are characterized by a weak to locally well developed parallel alignment of its mineral phases and the presence of rare amphibolite xenoliths. Locally, granodiorite intrudes along layering in the quartzite and quartz-mica schist. The dikes increase in size and abundance to the north toward the contact with a lithologically identical counterpart, the Selwyn gneiss, a sill-like body that intrudes foliation in the Nasina Series along the north margin of the study area (fig. 2). The dikes are interpreted to be satellite intrusions that emanated from the main intrusive body. The presence of foliated amphibolite xenoliths in granite and intrusion along tectonic layering in the Nasina series rocks indicates that intrusion postdated deformation and metamorphism of the Nasina series. A subsequent deformation event is required to explain the shearing and locally gneissic character of the granite.

Thermobarometry

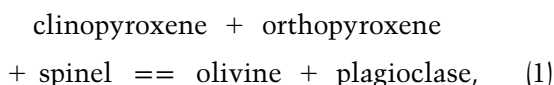
Cation-exchange geothermometers and TWQ multiequilibrium thermobarometry (Berman 1991) were applied to mineral chemical data of the orogenic peridotite body and its surrounding aureole to assess its pressure-temperature (PT) history (table 2). The two-pyroxene thermometer of Taylor (1998) records temperatures of ~1130°C for the peridotite samples. Other more commonly used two-pyroxene thermometers record temperatures of ~900°C. The latter temperatures compare well with those calculated using a Ca-in-orthopyroxene thermometer applied to orthopyroxene rims (Brey and Köhler 1990). In all samples, the Ca- and Al-rich orthopyroxene cores record temperatures ~50°–100°C greater than rims using any of the thermobarometers (table 2).

The Fe-Mg exchange temperatures ($T_{\text{Ol-Sp}}$) recorded by olivine and spinel extend to much lower values than two-pyroxene temperatures (900°–600°C). This is commonly observed in other orogenic peridotite massifs and is usually attributed to slow cooling during exhumation, with Fe-Mg exchange between olivine and spinel closing at a lower temperature than that for Ca and Al exchange between coexisting pyroxenes and spinel (Evans and Frost 1975; Ozawa 1983). Sample KE003

records a range in $T_{\text{Ol-Sp}}$ from 600° to 900°C that correlates with spinel grain sizes from 0.1 to 1.2 mm, respectively, further supporting reequilibration during slow cooling with larger grains closing to Fe-Mg diffusion at higher temperature (Ozawa 1983). Because the spinel in all samples is physically isolated from olivine by coronae of plagioclase, the $T_{\text{Ol-Sp}}$ could record Fe-Mg exchange between these two phases before growth of plagioclase coronae. This would require cooling prior to decompression. Alternatively, Fe-Mg exchange temperatures may record equilibration of spinel with neighboring olivine through the corona of plagioclase. Spinel has been shown to chemically communicate with olivine even when physically armored by pyroxene in slowly cooled ultramafic intrusions (Roeder and Campbell 1985), and it may have done so through plagioclase in these rocks if cooling and decompression during exhumation were coeval.

Physically touching grains of ortho- and clinopyroxene in the corona troctolite boudins record two-pyroxene temperatures of ~850°C. These temperatures are within uncertainty of those recorded by TWQ thermometry based on Fe-Mg exchange between coexisting pyroxenes and of those recorded by coexisting pyroxenes and large spinel grains in the adjacent peridotite body (table 2; fig. 5).

The development of plagioclase coronae on spinel records decompression of the peridotite body through the reaction



which defines the plagioclase-spinel peridotite facies boundary. The PT trajectory of reaction (1) does not depend critically on olivine composition but is affected considerably by plagioclase and spinel composition, with lower An content and more aluminous spinel displacing it to higher pressure (Green and Hibberson 1970). The position for reaction (1) in the peridotite was calculated using mineral chemical data and the TWQ method (fig. 5). The intersection of reaction (1) for the peridotite with T_{BKN} and $T_{\text{Ol-Sp}}$ on large spinel grains (table 2) suggests it decompressed to ~0.7 GPa at 800°–900°C (fig. 5).

Conversely, the growth of orthopyroxene and clinopyroxene coronae on olivine and plagioclase, respectively, in the troctolite boudins suggests these rocks have instead cooled rather than decompressed through reaction (1) (fig. 5). The position

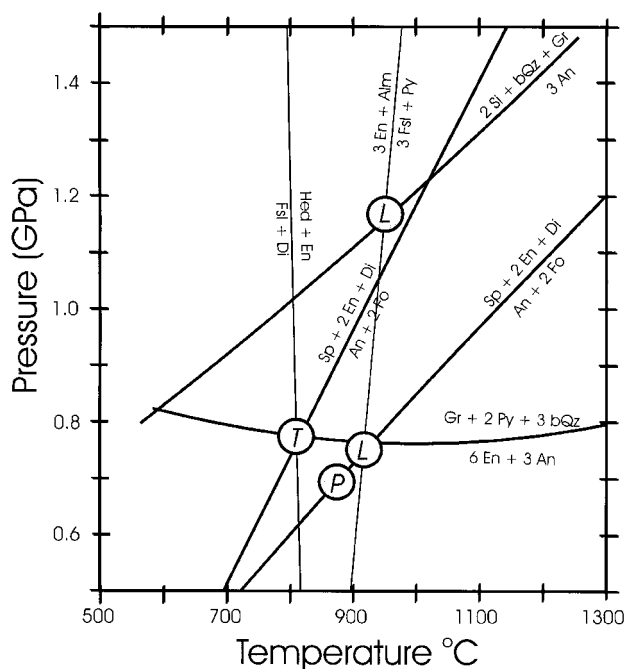


Figure 5. Diagram showing pressure and temperature conditions (*circles*) in the peridotite (*P*), troctolite (*T*), and metapelite leucosome (*L*) constrained by TWQ multi-equilibrium thermobarometry (Berman 1991) and cation exchange geothermometry (table 2).

for reaction (1) in the troctolites was calculated using mineral chemical data and the TWQ method by assuming an aluminous spinel was present. The Fe/Mg ratio of the latter phase was calculated from $KD_{\text{Ol-Sp}}^{\text{Fe-Mg}}$ at 800°C (Ballhaus et al. 1991) assuming a low Cr (Cr number of 0.05) for this mafic bulk composition. The intersection of reaction (1) in the troctolite samples with T_{BKN} or the Fe-Mg exchange temperature in pyroxenes indicate it cooled through conditions of 800°–900°C at ~0.8 GPa (fig. 5).

Touching grains of orthopyroxene and Ca-rich garnet rims in the leucosome of the aureole surrounding the peridotite record Fe-Mg exchange temperatures of ~900°C (fig. 5), similar to temperatures recorded in the peridotite body and troctolite boudins (table 2). Core compositions in the leucosome are clearly out of equilibrium. Pressures are more difficult to ascribe for this rock. Applying the garnet-plagioclase-quartz-sillimanite barometer to mineral chemical data for grain rims gives a pressure of ~1.2 GPa at the temperature recorded by garnet-orthopyroxene Fe-Mg exchange. In contrast, reactions not involving sillimanite give pressures of ~0.75 GPa, closer to those recorded by the pe-

ridotite and troctolite (fig. 5). In regions of biotite breakdown, plagioclase is not always present with garnet and sillimanite, and garnet is not always present with plagioclase and orthopyroxene (4A, 4B, 4D), so the pressure-dependent equilibria for this rock type in the aureole may not be reliable. Regardless, textures suggest garnet, sillimanite, and quartz formed with orthopyroxene as a result of biotite breakdown/melting to form the leucosome in the aureole (4D). This reaction has been experimentally measured in several pelites to be between 800° and 950°C at ~1.0 GPa (Gardien et al. 1995; Vielzeuf and Schmidt 2001), generally consistent with the conditions recorded by coexisting orthopyroxene and garnet in the leucosome and those of the immediately adjacent peridotite and troctolite bodies (fig. 5).

Geochemistry

Bulk chemical analyses performed on six samples from the Buffalo Pitts peridotite body (table 3; fig. 2B) show it to be homogeneous in bulk composition. The slight differences in Al₂O₃ content between samples may be attributed to variations in

the olivine/pyroxene ratio observed as centimeter-scale layering in outcrop, even though large samples (>500 g) were used to obviate this problem. Using Al₂O₃ as a depletion index, all six samples plot within the more fertile range of orogenic peridotites worldwide and of Cordilleran mantle sampled as xenoliths in Neogene volcanics throughout British Columbia and Yukon (fig. 6). The Buffalo Pitts peridotites are far more fertile than abyssal peridotite or subduction zone peridotites and plot within the range of mantle sampled by continental rift xenoliths or preoceanic rift margins such as the Zabargad massif in the Red Sea (Bonatti et al. 1986).

The Buffalo Pitts peridotites are enriched in incompatible elements, with rare earth element (REE) abundances near or above the upper part of the range for most orogenic peridotites at similar levels of depletion (fig. 7). Most notably, all the peridotites show light REE (LREE) enrichment relative to the heavy REE (HREE) and have either flat or steep negative patterns (fig. 7). Elevated LREE are observed in many mantle residues and may be due to enrichment by melt metasomatism in the mantle (McDonough and Frey 1990) or interaction of mantle lithosphere with fluids derived from adjacent

Table 3. Whole Rock and Re-Os Isotope Geochemistry

	BPP008	KE001	KE003	BPP009	DC004	DC005
Sample wt%:						
SiO ₂	45.8	45.9	45.2	45.6	45.9	45.8
TiO ₂	.10	.11	.11	.08	.10	.10
Al ₂ O ₃	3.51	3.24	3.11	2.72	3.43	3.06
FeO	7.66	8.24	8.18	8.48	8.22	8.29
MnO	.10	.11	.11	.11	.11	.11
MgO	40.3	39.9	40.2	41.5	39.8	40.2
CaO	2.04	2.45	2.76	1.52	2.31	2.08
Na ₂ O	.17	.11	.15	.08	.08	.11
K ₂ O	.01	.01	.01	.01	.01	.01
P ₂ O ₅	.01	.01	.01	.01	.01	.01
Loss on ignition:	9.31	9.18	7.42	9.73	9.39	9.27
Parts per billion:						
Os	4.16	3.35	4.1		3.08	3.06
Re	.323	.27	.38		.22	.22
¹⁸⁷ Re/ ¹⁸⁸ Os	.3729	.387	.4402		.348	.3459
¹⁸⁷ Os/ ¹⁸⁸ Os	.1264	.1297	.1290		.1326	.1436
±	.00008	.00013	.00006		.00015	.00039
TRD (Ga) ^a	.5		.1			

Note. Major element compositions determined on glass disks and pressed pellets using a Phillips PW1400 X-ray fluorescence spectrometer at McGill University, Montreal. All oxides were recalculated to 100% anhydrous, and Fe was recalculated as FeO. Trace elements determined using a VG PQIIS inductively coupled mass spectrometer at the University of Victoria. Powdered samples were dissolved in HF-HNO₃. Accuracy based on analysis of standard basalt BCR-2 is better than 10% for all elements listed. The complete methodology for Re and Os isotope analysis is given elsewhere (Selby and Creaser 2001; Creaser et al. 2002). Peridotite samples (>200 g) were crushed in a jaw crusher equipped with ceramic plates and ground to a fine powder in an agate mill. The powdered samples were spiked with a mixed ¹⁸⁵Re + ¹⁹⁰Os tracer solution and dissolved by the Carius tube method (240°C, 48 h). Os and Re were separated and purified by solvent extraction, microdistillation, and anion exchange chromatographic techniques. The Re and Os isotopic compositions were measured using negative thermal ionization mass spectrometry (Creaser et al. 1991; Völkening et al. 1991) on a Micromass Sector 54 mass spectrometer by static Faraday collector analysis. Total procedural blanks for Re and Os are less than 10 pg and 5 pg, respectively. Precision is listed at 2σ confidence level.

^a Minimum Re depletion ages (TRD) calculated using $\lambda = 1.6667 \times 10^{-11} \text{yr}^{-1}$ and a primitive mantle value with ¹⁸⁷Os/¹⁸⁸Os of 0.1296 and ¹⁸⁷Re/¹⁸⁸Os of 0.428 (Meisel et al. 2001).

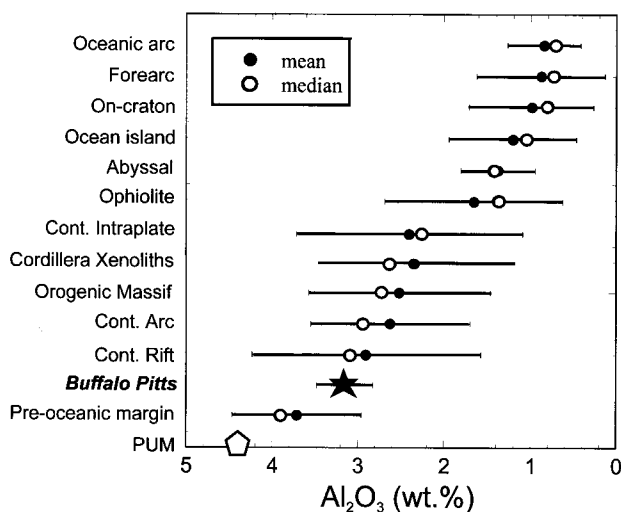


Figure 6. The median and mean level of depletion (Al_2O_3 content) of Buffalo Pitts peridotites (*star*) compared with peridotites in outcrop and xenoliths from various tectonic settings compiled from the literature ($n = 1200$). Also shown are estimated values for primitive upper mantle (PUM; McDonough and Sun 1995). Note the fertile nature of the Buffalo Pitts samples and other mantle peridotites from preoceanic or continental rift settings. Error bars are 1σ of the mean.

rocks during emplacement (Brueckner et al. 1988; Dupuy et al. 1991). The slight Eu anomalies exhibited by two samples (open symbols in fig. 7) are difficult to explain by any igneous mechanism. The Eu in these samples may have been affected by metamorphic fluids in equilibrium with plagioclase, perhaps from fluid-rock exchange with surrounding crustal rocks during exhumation. Similar disturbances of REE abundances have been reported in peridotites from the eastern Alps, the Trinity ophiolite, and Zabargad Island (Brueckner et al. 1988; Meisel et al. 1997; Gruau et al. 1998). In the two latter cases, the REE anomalies are thought to be due to exchange between peridotite and continental (meteoric) fluids in the surrounding country rocks as evidenced by Nd, Sr, and O isotopes.

Os isotopic compositions were measured in five peridotite samples (table 3) in an attempt to gain age information on the protoliths of these rocks. The contrasting compatibility of Re and Os during melt depletion leads to lower Re/Os (parent/daughter) in residues, and with time, these evolve to $^{187}\text{Os}/^{188}\text{Os}$ ratios that are below those of bulk earth. Due to the high concentrations of Os in ultramafic rocks, it has been assumed that $^{187}\text{Os}/^{188}\text{Os}$ ratios are less susceptible to change from mantle metasomatic processes or to alteration in the continen-

tal crust, compared to other radiogenic isotopic systems involving highly incompatible elements (Nd, Sr, Pb; Shirey and Walker 1998). Further work, however, has shown variable effects of metasomatism, serpentinization, or sea floor weathering on the Re-Os system (Meisel et al. 1997; Burnham et al. 1998; Snow et al. 2000; Schmidt and Snow 2002; Standish et al. 2002).

The Buffalo Pitts samples have a limited range of Re, Os, and Re/Os (table 3), consistent with the restricted range and level of depletion shown by their Al contents (fig. 6). The $^{187}\text{Os}/^{188}\text{Os}$ ratios of most of these samples are close to that estimated for primitive upper mantle (PUM; 0.1296[8]; Meisel et al. 1997) and are higher than is typical of other classic orogenic peridotites from the Alps and Pyrenees (Meisel et al. 2001). The high $^{187}\text{Os}/^{188}\text{Os}$ values are consistent with the high fertility of the Buffalo Pitts orogenic peridotite reflected in its major and trace element geochemistry (fig. 8).

Age relationships for orogenic peridotite bodies have been inferred from correlations of Os isotopes with Al (Reisberg and Lorand 1995). Samples from the Buffalo Pitts body show a near vertical array on an Os isotope–Al diagram (fig. 8), similar to peridotites from the Internal Ligurides of Italy (Snow et al. 2000). Sample DC005 is anomalously high in

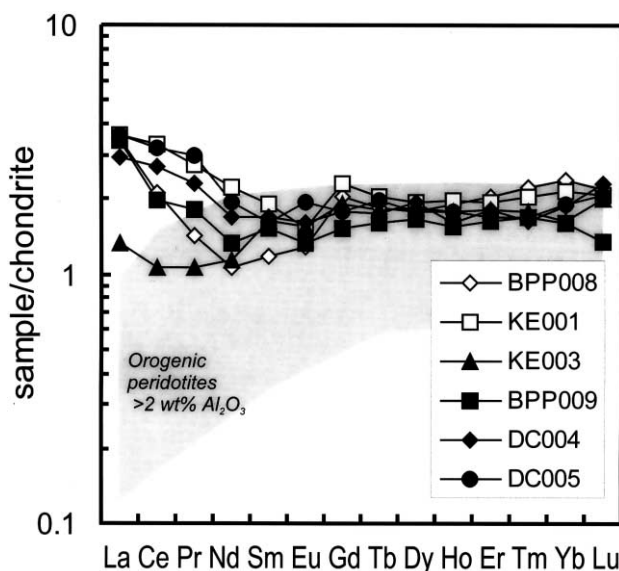


Figure 7. Rare earth element (REE) abundances in Buffalo Pitts peridotites normalized to chondrite using values of Anders and Grevesse (1989). Note the Eu anomalies in two samples (*open symbols*) and general light REE enrichment in most of the samples, relative to REE patterns for other orogenic peridotites with greater than 2 wt% Al_2O_3 (*shaded area*; McDonough and Frey 1990).

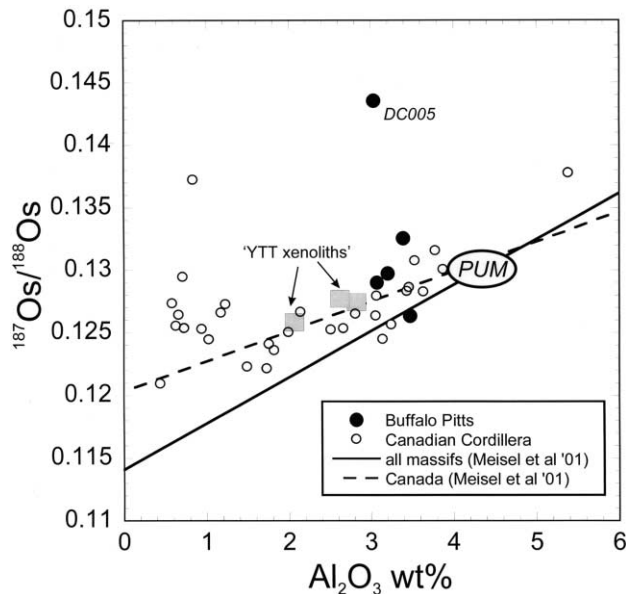


Figure 8. Covariation of Os isotopic ratios and with degree of depletion (measured by Al_2O_3) for the Buffalo Pitts peridotites, compared with data for northern Cordilleran spinel peridotite xenoliths (Peslier et al. 2000a, 2000b). The values for primitive upper mantle (PUM) and linear regressions from data compiled for all orogenic massifs (solid line) and mantle xenoliths from the Cordillera (dashed line) are from Meisel et al (2001). Note the anomalously high $^{187}\text{Os}/^{188}\text{Os}$ in sample DC005 and the similarity of most Buffalo Pitts samples to xenoliths hosted in Neogene volcanics erupted through the Yukon-Tanana Terrane (labeled “YTT xenoliths”).

$^{187}\text{Os}/^{188}\text{Os}$ (fig. 8), yet this sample is within meters of others (fig. 2B) and shows no significant petrographic or geochemical differences when compared to the other four samples. This scale of heterogeneity in Os isotopic composition is also recognized in the Horoman peridotite massif (Saal et al. 2001). Four of the five samples have unsupported $^{187}\text{Os}/^{188}\text{Os}$, having $^{187}\text{Os}/^{188}\text{Os}$ similar to or above chondritic values (~ 0.127) but with subchondritic $^{187}\text{Re}/^{188}\text{Os}$ (< 0.4 ; table 3). Superchondritic $^{187}\text{Os}/^{188}\text{Os}$ is observed in many other mantle samples and may be due to recent loss of Re (Meisel et al. 2001) or mobility of radiogenic Os of unknown origin, possibly seawater alteration (Standish et al. 2002) or interaction with crustal rocks (Schmidt and Snow 2002). Four samples plot along the trend of peridotite xenoliths sampled in Neogene volcanics from the northern Cordilleran mantle (fig. 8). The latter samples extrapolate to an initial $^{187}\text{Os}/^{188}\text{Os}$ ratio of 0.12, with an inferred model age of ~ 1 Ga (Peslier et al. 2000a, 2000b). The significance of this

age is questionable if Re, Os, or both isotopes are disturbed.

The Re and Os contents in the Buffalo Pitts samples show a good negative correlation with the level of LREE enrichment (table 3). Loss or gain of Re or Os may have occurred in the same events or by the same mechanisms which resulted in LREE enrichment in these peridotites, perhaps involving melt impregnation or interaction with crustal fluids during emplacement. These complications obscure any age inference for the body using Os isotope-Al correlations. Nonetheless, some estimate of the minimum age for formation of the Buffalo Pitts peridotite body can be made by calculating a Re depletion model age (T_{RD}) that measures the minimum age of lithosphere formation assuming all Re is exhausted during melting to produce a mantle residue (Shirey and Walker 1998). This approach, however, is applicable to only one of the five samples for which $^{187}\text{Os}/^{188}\text{Os}$ is statistically below that estimated for PUM. Sample BPP008 gives a T_{RD} of 0.5 ± 0.1 Ga. This poorly constrained Early Paleozoic age is similar to T_{RD} calculated for individual Cordilleran mantle xenoliths (Peslier et al. 2000a, 2000b) and to ages generally inferred for the Nasina series rocks of the Yukon-Tanana Terrane. It is older than Late Devonian and Early Mississippian mafic to felsic magmatism that characterizes the Yukon-Tanana Terrane (Mortensen 1992; Johnston and Hachey 1993), and that includes the Selwyn orthogneiss and other plutonic bodies that intrude the sequence of crustal rocks hosting the orogenic peridotite in the study area (fig. 2).

Discussion

Peridotite tectonite within metasedimentary units in the Yukon-Tanana Terrane are described along strike of the Buffalo Pitts region to the northwest in Alaska (Foster and Keith 1974; Keith et al. 1981; Foster et al. 1985). Most of these peridotite occurrences, however, are interpreted as fault-bounded tectonic slivers emplaced along fault systems with ages much younger than the Middle Paleozoic units which host the Buffalo Pitts peridotite (Foster et al. 1985). Indeed, no prior study has documented orogenic peridotite in an aureole of partially melted, granulite facies continental margin metasediments of the Yukon-Tanana Terrane as are recognized in Buffalo Pitts region.

Mineral textures and temperatures of equilibration of the Buffalo Pitts peridotite and its associated metamorphic aureole record their original equilibration conditions and exhumation path within this part of the Yukon-Tanana Terrane. The corona

of plagioclase around spinel grains in the peridotite body requires it to have originally existed at pressures above reaction (1) as a residue of limited partial melting. Original temperatures of greater than 1000°C are recorded by the Ca- and Al-rich cores of orthopyroxene (table 2), thus requiring a minimum pressure of origin of at least 0.9 GPa, likely in the mantle (figs. 5, 9). The peridotite body was then decompressed and cooled as evidenced by exsolution and development of Ca- and Al-poor rims in orthopyroxene grains, the formation of plagioclase coronae on spinel, and a relationship between T_{Ol-sp} and spinel grain size. Two-pyroxene temperatures of ~900°C record the temperature at which coexisting pyroxenes closed to diffusional exchange during decompression of the peridotite body to pressures below 0.7 GPa. Metastable spinel, assuming that it was able to exchange Fe and Mg with olivine through an armor of plagioclase, records further cooling of the body to ~600°C (fig. 9).

The metasedimentary and metaigneous rocks within the aureole approached conditions similar to the peridotite body (800°–900°C, 0.7–0.8 GPa; fig. 5) but along different *PT* paths. The troctolite boudins could be interpreted as hypabyssal intrusions that were transformed to two-pyroxene corona assemblages by tectonic burial. Alternatively, the boudins can be interpreted as structurally disrupted intrusive bodies in crust that cooled from *PT* conditions near the basalt solidus through reaction (1) at 850°C. The latter scenario is more consistent with all other field, petrographic, and geochemical data that point toward an extensional setting for the area. In contrast, unlike both the corona-textured peridotite and troctolite, the metapelite leucosome in the aureole texturally requires prograde heating to exceed the stability of biotite and partially melt at ~900°C (fig. 9). A nearly identical prograde metamorphic aureole is described in pelites adjacent to the Ronda orogenic peridotite (Loomis 1972a, 1972b) and is thought to be due to isobaric heating of the country rock by exhumation of a hot peridotite from the mantle during extensional unroofing of the Betic Cordilleras (Doblas and Oyarzun 1989; Platt and Vissers 1989).

Preservation of anhydrous mineralogies indicative of high *PT* conditions within regionally extensive quartzite and quartz-mica schist units typified by greenschist and amphibolite facies metamorphism may be linked to the structural position of the Buffalo Pitts peridotite in the immediate footwall of the thick Selwyn Gneiss (fig. 2). Regional deformation of the Yukon-Tanana Terrane postdating the emplacement of the peridotite body is indicated by the locally developed gneissic fabric in the in-

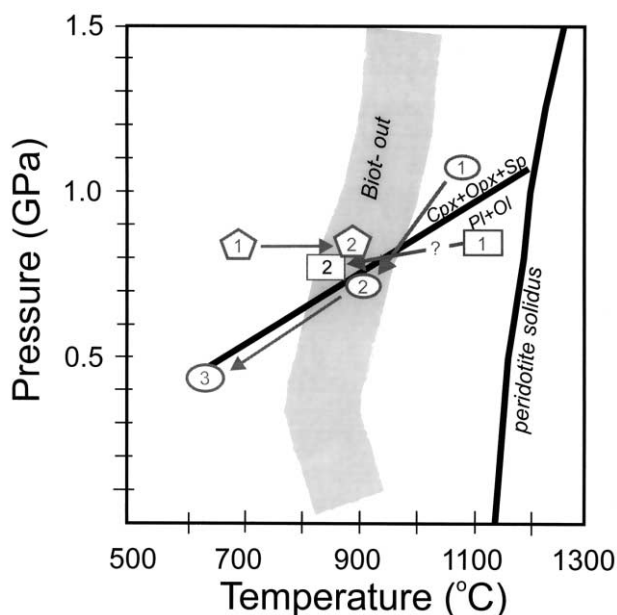


Figure 9. Diagram showing pressure-temperature history (labeled in sequence from 1 to 3) inferred for the peridotite (ovals), troctolite (squares), and metapelite aureole (polygons), based on thermobarometric (fig. 5; table 2) and textural (3, 4) constraints. Peridotite solidus from Hirschmann (2000). The subsolidus reaction $Ol + Pl = Cpx + Opx + Sp$ is based on the TWQ method (Berman 1991) applied to mineral chemical data from the peridotite samples (table 2). Temperature range for fluid-absent metapelite melting (shaded area, "Biot-out") is from a summary of experimental data (Vielzeuf and Schmidt 2001).

trusive Selwyn Gneiss. It may be that the peridotite body and its aureole were situated within a strain shadow that developed beneath this thick intrusive sheet during deformation and that prevented shearing and related retrograde metamorphism of the peridotite body and its surrounding aureole. Both the orogenic peridotite and troctolites were apparently strong lithologies that formed boudins on various scales within weaker quartzo-feldspathic lithologies of the aureole (figs. 2, 3D). Such a relationship has been proposed on a larger scale to explain the geological relationships for mantle peridotite bodies in the Ivrea Zone of the western Alps (Quick et al. 1995).

A structural origin for the peridotite and troctolite bodies as boudins requires significant stretching of the regional country rocks. Analogue experiments of stretching in a rheologically layered continental lithosphere have been used to explain the uplift and emplacement of upper mantle peridotite on the sea floor of passive continental mar-

gins (Brun and Beslier 1996). These experiments reproduce a remarkably identical juxtaposition of crustal and upper mantle lithologies as observed in the Buffalo Pitts region, albeit at a different scale. With increasing extension, stronger upper mantle lithologies are eventually boudinaged and uplifted to become tectonically juxtaposed against stronger, brittle upper crustal rocks. The analogue experiments of continental lithosphere rifting predict a scenario which explains the *PT* history and structural juxtaposition recorded by the Buffalo Pitts peridotite body and its country rocks.

Comparison with modern rifted margins and other well-studied orogenic peridotite bodies further strengthens a model of rifting of continental lithosphere for the formation and exhumation of the Buffalo Pitts peridotite body. The peridotite and its aureole share striking geological, petrographic, and geochemical similarities to the peridotite massifs from Zabargad and Ronda, which were emplaced during stretching of continental lithosphere to open the Red Sea and Alboran basins, respectively (Bonatti et al. 1986; Bonatti and Seyler 1987; Platt and Vissers 1989; Davies et al. 1993). First, the peridotites at Zabargad, Ronda, and Buffalo Pitts are all similarly structurally juxtaposed with metasediments and skarn in aureoles that underwent prograde metamorphism to granulite grade (Loomis 1972a; Bonatti et al. 1986; Bonatti and Seyler 1987; Boudier and Nicolas 1991). Second, like the Buffalo Pitts samples, the Zabargad peridotites show plagioclase coronae on spinel, recording exhumation across the spinel-plagioclase facies boundary during rifting and uplift. Third, both the Buffalo Pitts and Zabargad massifs show evidence of late-stage metasomatism (LREE enrichment) and are geochemically fertile when compared to mantle lithosphere from other tectonic settings, which typically show far higher levels of depletion (figs. 6, 7). Limited partial melt depletion is a signature of the preoceanic rift setting as observed for samples from the Zabargad massif (Bonatti and Michael 1989), the compositions of xenoliths from continental rifts (fig. 6) and a lack of significant volcanism within some rifted continental margins (Whitmarsh and Sawyer 1996).

If the Buffalo Pitts samples represent lithosphere formed during incipient rifting of continental lithosphere, then Os isotopic compositions may provide some broad constraints on the timing for such an episode within the Yukon-Tanana Terrane. The lack of ancient (>1.0 Ga) T_{RD} ages so commonly observed for the classic orogenic peridotite massifs in Europe (Meisel et al. 1997; Burnham et al. 1998) implies that the melt depletion and/or metaso-

matism of mantle lithosphere sampled by the Buffalo Pitts body occurred not long before its structural juxtaposition and exhumation within Devonian rifted margin sedimentary rocks (i.e., quartzites) of the Yukon Tanana terrane. Almost all $^{187}\text{Os}/^{188}\text{Os}$ ratios are within error of present-day bulk earth, indicating perhaps that the mantle lithosphere formed and was exhumed shortly thereafter during continental rifting. The only significant T_{RD} obtained (from sample BPP 008, at 0.5 Ga) does not differ substantially from the age of the crustal rocks which host this orogenic peridotite body, thus supporting this inference. If the lithosphere is juvenile, then the Re-Os isotopic systematics show that incipient rifting of the continental margin occurred in the Early Paleozoic. Subsequent to rifting, a magmatic arc was built upon this Early Paleozoic rifted continental margin, as evidenced by geochemical data from other crystalline rocks in the Dawson Range (Selby et al. 1999).

Mantle lithosphere in the Buffalo Pitts peridotite body and xenoliths in Neogene volcanic rocks erupted through this terrane have nearly identical Os isotopic compositions at a given degree of depletion (fig. 8). This similarity suggests that the crust and upper mantle were coupled in this terrane during Early Paleozoic continental rifting and have remained coupled well into the Neogene. If so, the Yukon-Tanana terrane would be a thick-skinned crustal block of coherent crust and mantle rather than a thin-skinned crustal flake that was scraped off and separated from its lithospheric mantle during accretion.

Although considered to have formed in a continental margin setting, evidence for a rifted margin origin for the Yukon-Tanana Terrane has been lacking. Results of this detailed study of the Buffalo Pitts orogenic peridotite and its host rocks provide the first direct evidence of lithospheric scale rifting involving the Yukon-Tanana Terrane. Mapping, petrological, and geochemical studies of the peridotite body and its aureole provide constraints on the conditions, processes, and mechanisms active during lithospheric stretching and the related emplacement of mantle rocks within the upper crust. In this light, the hundreds of other peridotite tectonite occurrences in this terrane (Foster and Keith 1974) may require further detailed examination and may similarly mark Early Paleozoic rifting and passive margin formation.

Conclusions

A megaboudin (~500 m) of orogenic peridotite is structurally interleaved with smaller boudined

masses and blocks (0.1–10 m) of corona-textured troctolite and skarn in continental margin rocks of the Yukon-Tanana Terrane, Yukon. The peridotite body records cooling and decompression from >1000°C and at least 0.9 GPa to ~850°C below the spinel-plagioclase peridotite facies reaction at 0.7 GPa. Two-pyroxene coronae in the troctolite boudins record cooling to 850°C through the identical reaction. Leucosome in a granulite facies aureole enveloping the peridotite body records prograde heating above the fluid-absent metapelite solidus to temperatures of ~900°C. The structural juxtaposition of upper mantle peridotite and troctolite boudins within an aureole of granulite-grade continental margin metasediments occurred during stretching of continental lithosphere at least 25 km thick in an Early Paleozoic preoceanic passive mar-

gin. Re-Os isotopic compositions of the peridotite body indicate that it may have formed as lithosphere with a similar or slightly older age than the rifted margin metasedimentary rocks into which it was exhumed.

ACKNOWLEDGMENTS

This study was supported financially by Natural Sciences and Engineering Research Council of Canada and Yukon Geology Program research grants to D. Canil and S. T. Johnston. J. Fan and M. Raudsepp are thanked for assistance with inductively coupled mass spectrometer and microprobe analyses, respectively. We especially thank K. Larson for able field assistance and E. Essene and D. G. Pearson for reviews.

REFERENCES CITED

- Anders, E., and Grevesse, N. 1989. Abundances of the elements: meteoric and solar. *Geochim. Cosmochim. Acta* 53:197–214.
- Ballhaus, C.; Berry, R. F.; and Green, D. H. 1991. High pressure experimental calibration of the olivine-orthopyroxene-spinel oxygen barometer: implications for the oxidation state of the upper mantle. *Contrib. Mineral. Petrol.* 107:27–40.
- Berman, R. G. 1991. Thermobarometry using multi-equilibrium calculations: a new technique, with petrological applications. *Can. Mineral.* 29:833–855.
- Bonatti, E., and Michael, P. J. 1989. Mantle peridotites from continental rifts to ocean basins to subduction zones. *Earth Planet. Sci. Lett.* 91:297–311.
- Bonatti, E.; Ottonello, G.; and Hamlyn, P. R. 1986. Peridotites from the island of Zabargad (St. John), Red Sea: petrology and geochemistry. *J. Geophys. Res.* 91:599–631.
- Bonatti, E., and Seyler, M. 1987. Crustal underplating and evolution of the Red Sea rift: uplifted gabbro-gneiss crustal complexes on Zabargad and Brothers Islands. *J. Geophys. Res.* 92:12,803–12,821.
- Boudier, F., and Nicolas, A. 1991. High-temperature hydrothermal alteration of peridotite, Zabargad Island (Red Sea). *J. Petrol. Spec. Lherzolites Issue*, p. 243–253.
- Brey, G., and Köhler, T. 1990. Geothermobarometry in four-phase lherzolites. II. New thermobarometers, and practical assessment of existing thermobarometers. *J. Petrol.* 31:1353–1378.
- Brueckner, H. K.; Zindler, A.; Seyler, M.; and Bonatti, E. 1988. Zabargad and the isotopic evolution of the sub-Red Sea mantle and crust. *Tectonophysics* 150:163–176.
- Brun, J. P., and Beslier, M. O. 1996. Mantle exhumation at passive margins. *Earth Planet. Sci. Lett.* 142:161–173.
- Burnham, O.; Rogers, N. W.; Pearson, D. G.; van Calsteren, P. W.; and Hawkesworth, C. J. 1998. The petrogenesis of the eastern Pyrenean peridotites: an integrated study of their whole rock geochemistry and Re-Os isotope composition. *Geochim. Cosmochim. Acta* 62:2293–2310.
- Creaser, R. A.; Papanastassiou, D. A.; and Wasserburg, G. J. 1991. Negative thermal ion mass spectrometry of osmium, rhenium and iridium. *Geochim. Cosmochim. Acta* 55:397–401.
- Creaser, R. A.; Sannigrahi, P.; Chacko, T.; and Selby, D. 2002. Further evaluation of the Re-Os geochronometer in organic-rich sediments: a test of hydrocarbon maturation effects in the Exshaw Formation, Western Canada Sedimentary Basin, Canada. *Geochim. Cosmochim. Acta* 66:3441–3452.
- Davies, G. R.; Nixon, P. H.; Pearson, D. G.; and Obata, M. 1993. Tectonic implications of graphitized diamonds from the Ronda peridotite massif, southern Spain. *Geology* 21:471–474.
- Den Tex, E. 1969. Origin of ultramafic rocks, their tectonic setting and history: a contribution to the discussion of the paper "The origin of ultramafic and ultrabasic rocks" by P. J. Wyllie. *Tectonophysics* 7:457–488.
- Dick, H. J. B., and Sinton, J. M. 1979. Compositional layering in Alpine peridotites: evidence for pressure solution creep in the mantle. *J. Geol.* 87:403–416.
- Doblas, M., and Oyarzun, R. 1989. "Mantle core complexes" and Neogene extensional detachment tectonics in the western Betic Cordilleras, Spain: an alternative model for the emplacement of the Ronda peridotite. *Earth Planet. Sci. Lett.* 93:76–84.
- Dupuy, C.; Mevel, C.; Bodinier, J.-L.; and Savoyant, L. 1991. Zabargad peridotite: evidence for multistage metasomatism during Red Sea rifting. *Geology* 19:722–725.
- Evans, B. E., and Frost, B. R. 1975. Chrome-spinel in progressive metamorphism: a preliminary analysis. *Geochim. Cosmochim. Acta* 39:959–972.

- Foster, H. L.; Cushing, G. W.; and Keith, T. E. C. 1985. Early Mesozoic tectonic history of the Boundary area, east-central Alaska. *Geophys. Res. Lett.* 12:553–556.
- Foster, H. L., and Keith, T. E. C. 1974. Ultramafic rocks of the Eagle quadrangle, east-central Alaska. *J. Res. U.S. Geol. Surv.* 2:657–669.
- Gardien, V.; Thompson, A. B.; Grujic, D.; and Ulmer, P. 1995. Experimental melting of biotite + plagioclase + quartz + muscovite assemblages and implications for crustal melting. *J. Geophys. Res.* 100:15,581–15,591.
- Green, D. H., and Hibberson, W. 1970. The instability of plagioclase in peridotite at high pressure. *Lithos* 3: 209–221.
- Gruau, G.; Bernard-Griffiths, J.; and Lecuyer, C. 1998. The origin of U-shaped rare earth patterns in ophiolite peridotites: assessing the role of secondary alteration and melt/rock reaction. *Geochim. Cosmochim. Acta* 62:3545–3560.
- Hirschmann, M. M. 2000. Mantle solidus: experimental constraints and the effects of peridotite composition. *Geochem. Geophys. Geosyst.*, vol. 1.
- Johnston, S. T. 1999. Large-scale coast-parallel displacements in the Cordillera: a granitic resolution to a paleomagnetic dilemma. *J. Struct. Geol.* 21:1103–1108.
- . 2001. The great Alaskan terrane wreck: reconciliation of paleomagnetic and geological data in the northern Cordillera. *Earth Planet. Sci. Lett.* 193: 259–272.
- Johnston, S. T., and Hachey, N. 1993. Preliminary results of 1 : 50 000 scale regional geological mapping in Wolverine Creek map area (115I/12), Dawson Range, southwest Yukon. *Yukon Explor. Geol.* 1992:49–60.
- Keith, T. E.; Foster, H. L.; Foster, R. L.; Post, E. V.; and Lehmbeck, W. L. 1981. Geology of an Alpine peridotite in the Mount Sorenson area, east central Alaska. *U.S. Geol. Surv. Prof. Pap.* 1170-A:A1–A9.
- Latin, D., and White, N. 1990. Generating melt during lithospheric extension: pure shear vs. simple shear. *Geology* 18:327–331.
- Loomis, T. P. 1972a. Contact metamorphism of pelitic rock by the Ronda ultramafic intrusion, southern Spain. *Geol. Soc. Am. Bull.* 83:2449–2474.
- . 1972b. Diapiric emplacement of the Ronda high-temperature ultramafic intrusion, southern Spain. *Geol. Soc. Am. Bull.* 83:2475–2496.
- McDonough, W., and Frey, F. A. 1990. Rare earth elements in upper mantle rocks. *In* Lipin, B. R., and McKay, G. A., eds. *Reviews in mineralogy*. Min. Soc. Am., Washington, D.C., p. 100–145.
- McDonough, W. F., and Sun, S. S. 1995. The composition of the earth. *Chem. Geol.* 120:223–253.
- Meisel, T.; Melcher, F.; Tomascak, P.; Dingeldey, C.; and Koller, F. 1997. Re-Os isotopes in orogenic massifs in the eastern Alps, Austria. *Chem. Geol.* 143:217–229.
- Meisel, T.; Walker, R. J.; Irving, A. J.; and Lorand, J. P. 2001. Osmium isotopic compositions of mantle xenoliths: a global perspective. *Geochim. Cosmochim. Acta* 65:1311–1323.
- Mortensen, J. K. 1992. Pre-mid-Mesozoic tectonic evolution of the Yukon-Tanana terrane, Yukon and Alaska. *Tectonics* 11:836–853.
- Ozawa, K. 1983. Evaluation of olivine-spinel geothermometry as an indicator of thermal history for peridotites. *Contrib. Mineral. Petrol.* 82:52–65.
- Peslier, A. H.; Reisberg, L.; Ludden, J.; and Francis, D. 2000a. Os isotopic systematics in mantle xenoliths: age constraints on the Canadian Cordillera lithosphere. *Chem. Geol.* 166:85–101.
- . 2000b. Re-Os constraints on harzburgite and lherzolite formation in the lithospheric mantle: a study of northern Cordillera xenoliths. *Geochim. Cosmochim. Acta* 17:3061–3071.
- Platt, J. P., and Vissers, R. L. M. 1989. Extensional collapse of thickened continental lithosphere: a working hypothesis for the Alboran Sea and Gibraltar arc. *Geology* 17:540–543.
- Quick, J. E.; Sinigoi, S.; and Mayer, A. 1995. Emplacement of mantle peridotite in the lower continental crust, Ivrea-Verbano zone, northwest Italy. *Geology* 23:739–742.
- Reisberg, L., and Lorand, J. P. 1995. Longevity of sub-continental mantle lithosphere from osmium isotope systematics in orogenic peridotite massifs. *Nature* 376:159–162.
- Roeder, P. L., and Campbell, I. H. 1985. The effect of post-cumulus reactions on composition of chrome spinels from the Jimberlana intrusion. *J. Petrol.* 26:763–786.
- Saal, A. E.; Takazawa, E.; Frey, F. A.; Shimizu, N.; and Hart, S. R. 2001. Re-Os isotopes in the Horoman Peridotite: evidence for refertilization? *J. Petrol.* 42: 25–37.
- Schmidt, G., and Snow, J. 2002. Os isotopes in mantle xenoliths from the Eifel volcanic field and the Vogelsberg (Germany): age constraints on the lithospheric mantle. *Contrib. Mineral. Petrol.* 143: 694–705.
- Selby, D., and Creaser, R. A. 2001. Re-Os geochronology and systematics of molybdenite from the Endako porphyry Mo deposit, British Columbia, Canada. *Econ. Geol.* 96:197–204.
- Selby, D.; Creaser, R. A.; and Nesbitt, B. E. 1999. Major and trace element compositions and Sr-Nd-Pb systematics of crystalline rocks from the Dawson Range, Yukon, Canada. *Can. J. Earth Sci.* 36:1463–1481.
- Shirey, S. B., and Walker, R. J. 1998. The Re-Os isotope system in cosmochemistry and high-temperature geochemistry. *Annu. Rev. Earth Planet. Sci.* 26: 423–500.
- Snow, J. E.; Schmidt, G.; and Rampone, E. 2000. Os isotopes and highly siderophile elements (HSE) in the Ligurian ophiolites, Italy. *Earth Planet. Sci. Lett.* 175: 119–132.
- Standish, J. J.; Hart, S. R.; Blustajn, J.; Dick, H. J. B.; and Lee, K. L. 2002. Abyssal peridotite osmium isotopic compositions from Cr-spinel. *Geochim. Geophys. Geosys. Paper* 2001GC000161, p. 1–24.
- Taylor, W. R. 1998. An experimental test of some geothermometer and geobarometer formulations for upper mantle peridotites with application to the ther-

- mobarometry of fertile lherzolite and garnet websterite. *Neues Jahrb. Mineral. Abh.* 172:381–408.
- Tempelman-Kluit, D. J. 1973. Reconnaissance geology of Aishihik Lake, Snag and part of Stewart River map areas, west-central Yukon. *Geol. Surv. Can. Pap.* 73-41, p. 93
- Vielzeuf, D., and Schmidt, M. W. 2001. Melting relations in hydrous systems revisited: application to metapelites, metagreywackes and metabasalts. *Contrib. Mineral. Petrol.* 141:251–267.
- Völkening, J.; Walczyk, T.; and Heumann, K. G. 1991. Osmium isotope ratio determinations by negative thermal ion mass spectrometry. *Int. J. Mass Spectrom.* 105:147–159.
- Wells, P. R. 1977. Pyroxene thermometry in simple and complex systems. *Contrib. Mineral. Petrol.* 62:129–139.
- Wernicke, B. 1985. Uniform-sense normal simple shear of the continental lithosphere. *Can. J. Earth Sci.* 22:108–125.
- Wheeler, J. O., and McFeeley, P. 1991. Tectonic assemblage map of the Canadian Cordillera and adjacent parts of the U.S.A. *Geol. Surv. Can. Map* 1712A, scale 1 : 2,000,000.
- Whitmarsh, R. B., and Sawyer, D. S. 1996. The ocean/continent transition beneath the Iberia abyssal plain and continental-rifting to sea floor spreading hypotheses. *In* Whitmarsh, R. S.; Sawyer, D. S.; Klaus, A.; and Masson, D. G., eds. *Proceedings of the Ocean Drilling Program, Scientific Results, Vol. 149*, College Station, Tex., p. 713–733.
- Witt-Eickschen, G., and Seck, H. A. 1991. Solubility of Ca and Al in orthopyroxene from spinel peridotite: an improved version of an empirical thermometer. *Contrib. Mineral. Petrol.* 106:431–439.